

Electron spin magnetism of zigzag graphene nanoribbon edge states

Kun Xu^{a)} and Peide D. Ye

School of Electrical and Computer Engineering and Birck Nanotechnology Center, Purdue University, West Lafayette, Indiana 47907, USA

(Received 16 January 2014; accepted 11 April 2014; published online 22 April 2014)

The electron spin states of zigzag graphene nanoribbon (ZGNR) edge play a pivotal role in the applications of graphene nanoribbons. However, the exact arrangements of the electron spins remain unclear to date. In this report, the electronic spin states of the ZGNR edge have been elucidated through a combination of quantum chemical investigation and previous electron spin resonance experiment observations. An alternating α and β spin configuration of the unpaired electrons along the ZGNR edge is established in ambient condition without any external magnetic field, and the origin of the spin magnetism of the ZGNR edge is revealed. It paves a pathway for the understanding and design of graphene based electronic and spintronic devices. © 2014 AIP Publishing LLC. [<http://dx.doi.org/10.1063/1.4872377>]

With remarkable electronic, optical, mechanical and thermal properties, graphene has become the center of attention in the field of material research over the past decade.¹ The zigzag graphene nanoribbons (ZGNRs) are recognized to be a good target material for the future electronics and spintronics devices owing to the long spin-relaxation times and lengths.^{2,3} Recently, nano-graphene with zigzag edges was observed by scanning tunneling microscopy (STM) and the localized states at the zigzag edge were confirmed by spectroscopy scanning tunneling.⁴⁻⁶ When the zigzag edge is formed by bisecting the C–C σ bonds, the ZGNR possesses dangling σ bonds of sp^2 type on the edge carbon atoms.³ There is an unpaired electron in each of these σ orbitals. While it is known that the magnetic properties of ZGNR directly pertains to the electronic spin states of its edge carbon atoms, the spin orientations of the electrons along the ZGNR edge have yet to be clarified.⁷⁻¹⁰

Recently, three experiments⁸⁻¹⁰ evidenced the existence of the magnetism of ZGNR edge by magnetic measurements, as well as the localized spin of the unpaired electrons at the ZGNR edge confirmed by electron spin resonance (ESR) measurements.⁹⁻¹¹ By tight binding band calculations on ZGNR, Fujita *et al.*¹² proposed a local ferrimagnetic ordering along the ZGNR edge and anti-parallel magnetic moments localized at opposite edges across the ZGNR. It signifies that electrons with α spin (up-spin) are concentrated on one zigzag edge of ZGNR and equivalent β spin (down-spin) on the opposite zigzag edge. Therefore, the total magnetization of the ZGNR is expected to be zero. Based on this theoretical prediction, the authors of abovementioned experiments speculated that the possible origin of the magnetism of ZGNR comes from the symmetry-breakage or defects, which would cause the unequal number of the α spins and the β spins among ferrimagnetically ordered edge states. At first glance this proposition is seemingly sound. However, it cannot explain a recent experiment carried out by Rao *et al.*¹³ who reported through ESR measurements that the ground state $O_2(^3\Sigma^-_g)$ not only can be adsorbed at the ZGNR edges easily

at $T = 300$ K and $P_{O_2} = 1420$ Torr but also can be desorbed completely with vacuum treatment at the temperature of 293 K. The prediction theorized by Fujita *et al.* would render the process of complete desorption impossible due to the large adsorption energy of about 5 eV. As illustrated in Figure 1, both oxygen atoms from $O_2(^3\Sigma^-_g)$ can attach to two adjacent carbon radicals of ZGNR edge, according to previously proposed edge spin arrangements, making this complex too strong for the oxygen atoms to be desorbed from the ZGNR edge. This obvious contradiction led us to reexamine the electronic spin configuration and the origin of magnetism of ZGNR edge. We will see in the following discussions, how alternating anti-parallel spins (resembling a one-dimensional antiparallel chain along an individual edge), although slightly higher in energy, might appear at the ZGNR edge.

The ZGNR edge is reminiscent of a multi-radical boundary, since each carbon atom of the ZGNR edge has a dangling σ bond. Here, we consider two possible electronic states of ZGNR edge atoms: (1) aligning the unpaired electrons in same spin orientation, the same as in the prediction of Fujita *et al.*, and (2) an alternating α and β spin orientations along the edge of ZGNR. To determine what the exact electron spin configuration is at the ground state of ZGNR, we first compared the singlet and triplet electronic state energies of four radical models, $C_{10}H_6$, $C_{18}H_8$, $C_{28}H_{12}$, and $C_{28}H_{10}$, as shown in Table I, which were calculated at the CAS, CIPT2, and B3LYP levels of quantum chemical theory.¹⁴⁻¹⁶ It can be seen that the energy at triplet state is slightly lower than that at the singlet state. At the B3LYP level, the differences ($\Delta E_{st} = E_{\text{triplet}} - E_{\text{singlet}}$) are predicted to be -0.0015 , -0.0214 , and -0.0081 eV for $C_{18}H_8$, $C_{28}H_{12}$, and $C_{28}H_{10}$, respectively. For models of two smaller clusters, $C_{10}H_6$ and $C_{18}H_8$, ΔE_{st} are predicted to be -0.0283 and -0.0224 eV at the CAS level, and -0.0167 and -0.0247 eV at the CIPT2 level. $C_{18}H_8$ and $C_{28}H_{10}$ with four carbon atom radicals have a small singlet-triplet split energy that is less than about 0.01 eV. The results are consistent with the 0.030 eV from Konishi *et al.*¹⁷ and 0.025 eV from Pisani *et al.*¹⁸ These imply that the transition from triplet state to singlet state is instantaneous due to the very small singlet-triplet split energy. Consequently, it is possible that the alternating α and β spin singlet state of ZGNR edge could act as a ground

^{a)} Author to whom correspondence should be addressed. Electronic mail: xu83@purdue.edu

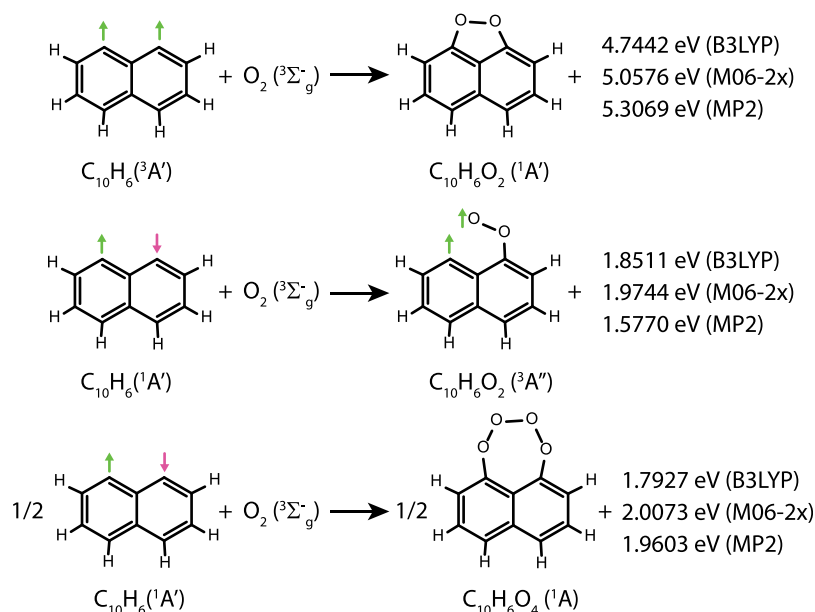


FIG. 1. Reaction diagrams of $O_2(^3\Sigma_g^-)$ with $C_{10}H_6$ and calculated spin density of edge carbon atoms in $C_{28}H_{10}(^1A)$. (a) Adsorption reactions diagram for $O_2(^3\Sigma_g^-)$ with different configurations of $C_{10}H_6$, and their associated adsorption energy at different levels of theory. Green and magenta arrows represent α and β orientations.

state and could conveniently transform into parallel spin configuration in an external magnetic field and exhibit paramagnetism.

As we have briefly mentioned before, the experiment of Rao *et al.*¹³ reported the behavior of both adsorption and desorption of oxygen molecules at the edge of ZGNR observed by means of ESR spectroscopy. Their observation shows that a chemical adsorption between oxygen molecule and ZGNR edge occurs to quench the ESR signal of the unpaired electrons of ZGNR edge due to the formation of the C–O bond.

This fully reversible process in ambient condition indicates that the chemical adsorption is relatively weak. Thus, a critical clue is given to us to uncover the spin configuration of ZGNR edge states through the careful scrutiny of the adsorption mechanism.

We have considered both $C_{10}H_6(^3A')$ and $C_{10}H_6(^1A')$ models for the $O_2(^3\Sigma_g^-)$ molecule adsorption mechanism at three levels (B3LYP, M06-2x, and MP2) of theory, as shown in Figure 1. $C_{10}H_6(^3A')$ designates the configuration in which adjacent carbon radicals of the ZGNR edge with

TABLE I. Comparison of energies of radical model systems calculated by CAS, CIPT2, and UB3LYP. E_s and E_t represent the energies of singlet and triplet radicals in hartree and $\Delta E_{st}(=E_t - E_s)$ in eV.

Graphene cluster	Method	E_s (hartree)	E_t (hartree)	ΔE_{st} (eV)
$C_{10}H_6$ 	CAS(8,10)/6–311G(d,p)	–382.194698	–382.195737	–0.0283
	CIPT2(8,10)/6–311G(d,p)	–383.443192	–383.443806	–0.0167
	UB3LYP/6–311G(d,p)	–384.605581	–384.605229	0.0096
$C_{18}H_8$ 	CAS(10,10)/6–31G(d)	–686.088136	–686.088958	–0.0224
	CIPT2(8,10)/6–311G(d,p)	–383.443192	–383.443806	–0.0247
	UB3LYP/6–311G(d,p)	–690.5622338	–690.5622816	–0.0015
$C_{28}H_{10}$ 	UB3LYP/6–311G(d,p)	–1074.360543	–1074.361331	–0.0214
$C_{28}H_{12}$ 	UB3LYP/6–311G(d,p)	–1072.978973	–1072.979269	–0.0081

parallel spins on the unpaired electrons. It can capture both O atoms of the $O_2(^3\Sigma_g^-)$ molecule simultaneously to form the singlet state peroxide $C_{10}H_6O_2(^1A')$ with the adsorption energies of 4.7442, 5.0576, and 5.3069 eV at the B3LYP, M06-2x, and MP2 levels, respectively. $C_{10}H_6(^1A')$ represents the second ZGNR edge configuration in which adjacent carbon radicals of the ZGNR edge have electrons with spins oriented in an anti-parallel fashion. As a result of the spin repulsion of the dangling O atom with the adjacent carbon radical, only one O atom of the $O_2(^3\Sigma_g^-)$ molecule is allowed to approach the ZGNR edge carbon radical to form the triplet state peroxide $C_{10}H_6O_2(^3A'')$. The adsorption energies of this process are 1.8511, 1.9744, and 1.5770 eV at the B3LYP, M06-2x, and MP2 levels. Next, because of the matching spins of the two dangling O atoms of the adjacent carbon positions, they can adjoin to form a singlet state tetra-oxide $C_{10}H_6O_4(^1A)$ with a $-O-O-O-O-$ structure. The adsorption energy binding one oxygen molecule in $C_{10}H_6O_4(^1A)$ is comparable to that in $C_{10}H_6O_2(^3A'')$. Namely, the formation of $C_{10}H_6O_4(^1A)$ does not increase the O-C bond strength. Hence, the $-O-O-O-O-$ structure is unstable. However, its formation gives rise to the disappearance of the ESR signal.

In comparison, the adsorption energy of $C_{10}H_6O_2(^1A')$ is about 5 eV, around 2.5 times greater than that of $C_{10}H_6O_2(^3A'')$ (or $C_{10}H_6O_4(^1A)$). In order to verify this result, a larger cluster model, $C_{28}H_{12}$, was calculated at the B3LYP and M06-2x levels of theory. As seen in Figure S1 in supplementary material,¹⁹ the adsorption energies at B3LYP and M06-2x are 1.9556 and 2.1106 eV for $C_{28}H_{12}O_2(^3A'')$, and 4.6270 and 4.9064 eV for $C_{28}H_{12}O_2(^1A')$, which are almost identical to the results using the $C_{10}H_6$ model.

With the geometries, frequencies, and adsorption energies of the $C_{28}H_{12}$ model with O_2 , the adsorption critical pressures at 293 K are estimated by statistical thermodynamics to be 14.96 Torr for the $C_{28}H_{12}O_2(^3A'')$ \rightarrow $C_{28}H_{12}(^1A') + O_2(^3\Sigma_g^-)$ process and 1.91×10^{-41} Torr for the $C_{28}H_{12}O_2(^1A')$ \rightarrow $C_{28}H_{12}(^3A'') + O_2(^3\Sigma_g^-)$ process. Without doubt, the first desorption process can readily occur at any pressure below 14.96 Torr, while the latter is forbidden as 1.91×10^{-41} Torr is beyond the highest achievable vacuum in any laboratory. Therefore, although the ESR signals of both parallel spin and anti-parallel spin states of ZGNR edges can be quenched by capturing of $O_2(^3\Sigma_g^-)$, only the alternating spin configuration of ZGNR edge states permits the total desorption of $O_2(^3\Sigma_g^-)$ from the adsorption complex. Hence, it supports the argument that the ZGNR edge consists of an anti-parallel arrangement at room temperature where the alternating α and β spin configuration is the ground state.

The anti-parallel spin configuration of the ZGNR edge states is demonstrated by the spin density isosurface of $C_{28}H_{10}(^1A)$ in Figure 2, in which the α and β spin densities distribute in an alternating manner on the vertices of the hexagons along the ZGNR edge. In Table SII of the supplementary material,¹⁹ we can see that the α and β orbitals in the frontier occupied molecular orbitals HOMO (Highest Occupied Molecular Orbital)-3 and HOMO-4 are almost localized at alternate sites of the ZGNR edge. It seems that the sp^2 orbitals are the dominate components of HOMO-3 and HOMO-4. Each unpaired electron (α or β) occupies one

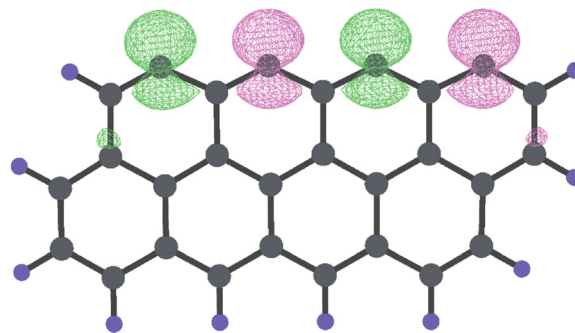


FIG. 2. Spin density isosurface of $C_{28}H_{10}(^1A)$ at 0.01. Green and magenta represent α and β spin density.

lobe of the sp^2 orbital in the plane of graphene. This supports the experimental results carried out by Tao *et al.*,²⁰ who indirectly inferred the localized electron density of state of the carbon atoms of ZGNR edge by STM. Due to this electronic configuration of ZGNR edge states, they exhibit particular chemical and electromagnetic properties that differ from the in-plane carbon atoms.

In conclusion, the edge states of ZGNR have been investigated by first-principles quantum chemical calculations. The results, when juxtaposed with prior experimental observations, have revealed insight into the electron spin magnetism at ZGNR edge. Calculations show that the singlet-triplet split energy of the ZGNR edge atoms is insignificant (<0.01 eV), implying the parallel and antiparallel spin configurations of the ZGNR edge can be interchangeable with an external field. Under ambient condition, the spin configuration of ZGNR edge appears to be antiparallel with alternating α and β spins. This allows the adsorption and complete desorption of $O_2(^3\Sigma_g^-)$ at ZGNR edge. With the introduction of an external magnetic field, spin configuration along the ZGNR edge may transform from antiparallel to parallel, and the material displays paramagnetism. Not only is the understanding of the electron spin magnetic behavior of ZGNR edge states crucial for the characterization of graphene based devices, it also opens routes for the research and development of graphene based electronic and spintronic devices.

¹A. K. Geim and K. S. Novoselov, *Nat. Mater.* **6**, 183 (2007).

²T. Enoki and Y. Kobayashi, *J. Mater. Chem.* **15**, 3999 (2005).

³D. Jiang, B. G. Sumpter, and S. Dai, *J. Chem. Phys.* **126**, 134701 (2007).

⁴Y. Niimi, T. Matsui, H. Kambara, K. Tagami, M. Tsukada, and H. Fukuyama, *Phys. Rev. B* **73**, 085421 (2006).

⁵C. Ö. Girit, J. C. Meyer, R. Erni, M. D. Rossell, C. Kisielowski, L. Yang, C.-H. Park, M. F. Crommie, M. L. Cohen, S. G. Louie, and A. Zettl, *Science* **323**, 1705 (2009).

⁶X. Jia, M. Hofmann, V. Meunier, B. G. Sumpter, J. Campos-Delgado, J. M. Romo-Herrera, H. Son, Y.-P. Hsieh, A. Reina, J. Kong, M. Terrones, and M. S. Dresselhaus, *Science* **323**, 1701 (2009).

⁷M. Acik and Y. J. Chabal, *Jpn. J. Appl. Phys.* **50**, 070101 (2011).

⁸Y. Wang, Y. Huang, Y. Song, X. Zhang, Y. Ma, J. Liang, and Y. Chen, *Nano Lett.* **9**, 220 (2009).

⁹V. L. Joly, M. Kiguchi, S.-J. Hao, K. Takai, T. Enoki, R. Sumii, K. Amemiya, H. Muramatsu, T. Hayashi, Y. A. Kim, M. Endo, J. Campos-Delgado, F. López-Urías, A. Botello-Méndez, H. Terrones, M. Terrones, and M. S. Dresselhaus, *Phys. Rev. B* **81**, 245428 (2010).

¹⁰S. S. Rao, S. N. Jammalamadaka, A. Stesmans, V. V. Moshchalkov, J. van Tol, D. V. Kosynkin, A. Higginbotham-Duque, and J. M. Tour, *Nano Lett.* **12**, 1210 (2012).

¹¹S. S. Rao, A. Stesmans, J. van Tol, D. V. Kosynkin, A. Higginbotham-Duque, W. Lu, A. Sinitskii, and J. M. Tour, *ACS Nano* **6**, 7615 (2012).

- ¹²M. Fujita, K. Wakabayashi, K. Nakada, and K. Kusakabe, *J. Phys. Soc. Jpn.* **65**, 1920 (1996).
- ¹³S. S. Rao, A. Stesmans, K. Keunen, D. V. Kosynkin, A. Higginbotham, and J. M. Tour, *Appl. Phys. Lett.* **98**, 083116 (2011).
- ¹⁴H.-J. Werner and P. J. Knowles, *J. Chem. Phys.* **82**, 5053 (1985).
- ¹⁵P. Celani, H. Stoll, H.-J. Werner, and P. J. Knowles, *Mol. Phys.* **102**, 2369 (2004).
- ¹⁶B. Miehlich, A. Savin, H. Stoll, and H. Preuss, *Chem. Phys. Lett.* **157**, 200 (1989).
- ¹⁷A. Konishi, Y. Hirao, K. Matsumoto, H. Kurata, R. Kishi, Y. Shigeta, M. Nakano, K. Tokunaga, K. Kamada, and T. Kubo, *J. Am. Chem. Soc.* **135**, 1430 (2013).
- ¹⁸L. Pisani, J. A. Chan, B. Montanari, and N. M. Harrison, *Phys. Rev. B* **75**, 064418 (2007).
- ¹⁹See supplementary material at <http://dx.doi.org/10.1063/1.4872377> for the details of the models and methods used.
- ²⁰C. Tao, L. Jiao, O. V. Yazyev, Y.-C. Chen, J. Feng, X. Zhang, R. B. Capaz, J. M. Tour, A. Zettl, S. G. Louie, H. Dai, and M. F. Crommie, *Nat. Phys.* **7**, 616 (2011).